Experimental Assessment of Adaptive Spatial Combining for Underwater Acoustic Communications

Guosong Zhang
Dept. of Elec. and Telecomm.
Norwegian Univ. of Sci. and Tech.
7491 Trondheim, Norway
Guosong.Zhang@iet.ntnu.no

Jens M. Hovem
SINTEF ICT
Norwegian Univ. of Sci. and Tech.
7491 Trondheim, Norway
Jens.Martin.Hovem@sintef.no

Hefeng Dong
Dept. of Elec. and Telecomm.
Norwegian Univ. of Sci. and Tech.
7491 Trondheim, Norway
Hefeng.Dong@iet.ntnu.no

Abstract— **This paper presents a receiver structure of passive-phase conjugation (PPC) based adaptive spatial combining for underwater acoustic communications. Based on temporal diversity exploited by PPC processing, the presented structure exploits spatial diversity by adaptive multichannel combining. The structure was assessed in two field experiments which were conducted in two different seasons in Trondheim harbor. The experiments were carried out with the same configuration, but the channel physics were different due to different environmental conditions. A cross receiving array of 10 hydrophones, deployed in a water depth of 10 m, was used to collect the received waveform in a range of 2.0 km. By off-line signal processing, we have demonstrated the superior performance in exploiting spatial diversity for underwater communications.**

Keywords- adaptive spatial combining; passive time reversal; passive-phase conjugation; underwater communication;spatial diversity.

I. INTRODUCTION

Underwater acoustic communication is frequently limited by intersymbol interference (ISI) due to a time-varying extended multipath structure in an acoustic channel [1]. Time delayed arrivals due to multipath propagation can be spatial and temporal refocused by time reversal method [2, 3], which mitigates ISI caused by multipath. After the equal weight multichannel combining, there is only one channel equalizer required by passive time reversal communications [4, 5], which can be realized by passive-phase conjugation (PPC). PPC achieves pulse compression for the time delayed arrivals [6], and this property is used for underwater acoustic communications with a reduced number of taps for adaptive channel equalization.

With multiple receivers distributed in space, there is spatial diversity which could be used to avoid deep fading in communications [7]. It is necessary to use multiple receivers in a time-varying acoustic channel to achieve stable communications. Since ISI cannot be eliminated by refocusing, an adaptive channel equalizer is required. It is known that a decision feedback equalizer (DFE) removes residual ISI. Spatial diversity is exploited by passive time reversal to mitigate ISI [8], where the side lobe level of $q(t)$ -function is reduced with an increased number of receivers. Multichannel combining is performed by passive time reversal to achieve refocusing at the receiving array. In a real ocean environment, since there are interchannel correlations among the receivers [9], the diversity combining of passive time reversal does not take spatial coherence into account.

In this paper, a receiver structure which is a PPC based multichannel equalization scheme is presented, where adaptive spatial combining is conducted to exploit spatial diversity. The structure takes advantage of pulse compression, where the number of taps for a multichannel equalizer is significantly reduced. As discussed by Yang [9], there is lack of model which can precisely predict the channel characteristics in a real ocean, and therefore the receiver structure is assessed by experiments. Two sea experiments were conducted to assess the receiver structure, where a receiving array of 10 hydrophones was used, and the received waveforms were recorded for off-line processing in the laboratory. The structure of PPC based multichannel DFE (PPC-McDFE) is used in digital signal processing, and it improves performance of the passive time reversal structure which is realized by PPC plus a signal channel DFE (PPC-DFE). The improvement is shown in terms of output signal-to-noise ratio (SNR).

This paper is organized as follows. The proposed receiver structure of PPC-McDFE is introduced in Section II, and the diagram shows its differences from PPC-DFE. Section III describes the experimental setup. The information about experimental area and sound speed profiles are shown, and the signal transmission is introduced. In Section IV, the channel measurements and communication results are presented and discussed. Conclusions are given in Section V.

II. THE RECEIVER STRUCTURE

The communication information consists of a sequence of symbols denoted as $I[n]$, and each symbol occupies a duration of T . The baseband data signal $s(t)$ can be expressed as

$$s(t) = \sum_n I[n] g(t - nT) \quad (1)$$

where $g(t)$ is the pulse shape function for each symbol such that

$$g(\tau)=\begin{cases}1, \text{for } 0\le\tau<T\\ 0, \text{otherwise}\end{cases}. \quad (2)$$

At the *i*th receiver, the received signal $r_i(t)$ can be written as

$$r_i(t)=h_i(t)\otimes s(t)+w_i(t) \quad (3)$$

where $h_i(t)$ represents the channel impulse response, $w_i(t)$ is a band-limited noise, and $\otimes$ denotes convolution. PPC processing can be seen as match-filtering of the received data signal using a channel response. The output of PPC is expresssed as

$$\begin{aligned} z_i(t) &= h_i(-t)\otimes r_i(t)\\ &= h_i(-t)\otimes\left(h_i(t)\otimes s(t)+w_i(t)\right)\\ &= q_i(t)\otimes s(t)+\varsigma_i(t), \end{aligned} \quad (4)$$

where $q_i(t)$ is the autocorrelation function of $h_i(t)$, and $\varsigma_i(t)$ is a filtered noise. The main lobe width and side lobes of $q_i(t)$ are determined by the channel physics, and ISI caused by $q_i(t)$ exists after pulse compression.

ISI can be mitigated by refocusing time delayed arrivals at a receiving array, where one channel output is obtained by passive time reversal. The output of diversity combining over *K* receivers is

$$\begin{aligned} z(t) &= \sum_{i=1}^{K} h_i(-t)\otimes r_i(t)\\ &= \sum_{i=1}^{K} q_i(t)\otimes s(t)+\sum_{i=1}^{K}\varsigma_i(t)\\ &= q(t)\otimes s(t)+\varsigma(t) \end{aligned} \quad (5)$$

where $q(t)$ is a function of autocorrelations summed over the *K* receivers, and $\zeta(t)$ is a filtered noise. Residual ISI caused by $q(t)$ can be removed by an adaptive channel equalizer [5]. Figure 1 shows the receiver structure for communications using passive time reversal, and it is realized by PPC plus a single channel DFE (PPC-DFE). Carrier-phase tracking is realized using the technique of a second order digital phase-locked loop (DPLL) proposed by Stojanovic [10], and the DPLL tracks the mean frequency shift of *K* receivers. Based on the minimum mean square error (MSE) criterion, the coefficients for the feed-forward and feedback filters are obtained by the recursive least squares (RLS) algorithm [11]. The output error is defined as

$$e[n]=I[n]-\tilde{I}[n] \quad (6)$$

where $\tilde{I}[n]$ is the estimate. Out the training mode, $I[n]$ is replaced by the decided output $\hat{I}[n]$.

The receiver structure PPC-McDFE is shown in Figure 2, and it takes advantage of pulse compression in order to reduce the number of taps for the multichannel DFE. For the K receivers, independent DPLLs compensate the frequency shifts, and the RLS algorithm updates coefficients of the feed-forward filters. This structure is designed to improve the performance of PPC-DFE by adaptive multichannel combining. As shown in Figure 1, one channel output exploits spatial diversity by low-complex combining without considering both the interchannel correlations and the output errors. For the structure shown in Figure 2, spatial diversity is exploited by performing adaptive spatial combining. Based on a previous output MSE, the RLS algorithm updates the filter tap coefficients for combining in order to minimize current output MSE. PPC-McDFE achieves superior performance in the trials.

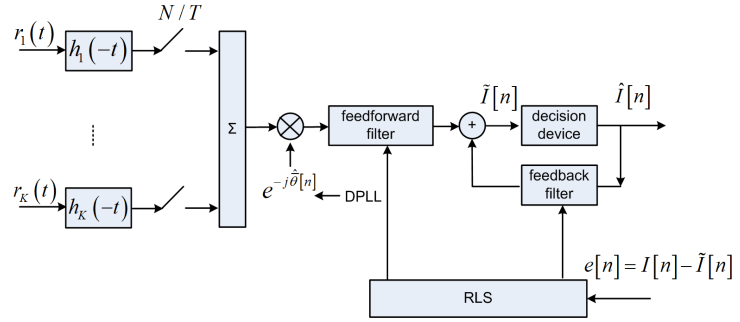

Figure 1. The diagram of PPC-DFE. There are *N* samples per symbol in baseband digital signal processing.

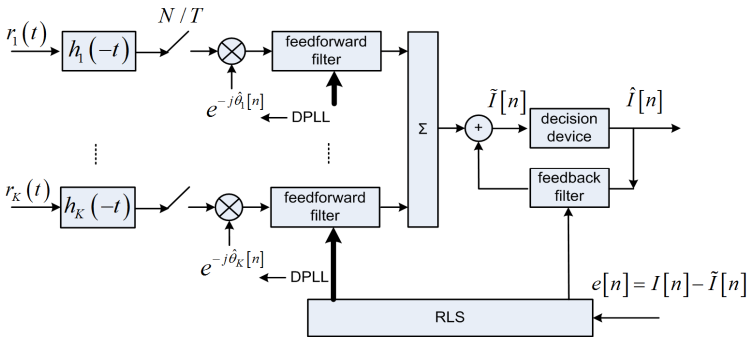

Figure 2. The diagram of PPC-McDFE.

III. THE EXPERIMENTS

The two experiments were carried out on June 30 (Trial A) and September 9 (Trial B), 2010, in Trondheim harbor in Norway shown in Figure 3(a). In the experimental area, the shallow littoral region less than 20 m extends about 100 m off shore. The instrumentation and the source sound level were the same for both Trial A and Trial B. Figure 3(b) shows that the depth profile from the source to the CRA changes from 240 m to 10 m. The red dot denotes the position of the transmitter in a distance of 2 km to the CRA, and the transmitter used a hemispherical acoustic transducer suspended at a depth of 20 m from the NTNU research vessel R/V Gunnerus. The CRA is near-shore deployed in a water depth of 10 m, and it consists of a vertical receiving array of 6 hydrophones with 1 m element spacing and a horizontal receiving array of 4 hydrophones with 1.5 m element spacing. The dynamic positioning system of R/V Gunnerus was activated to reduce drifting.

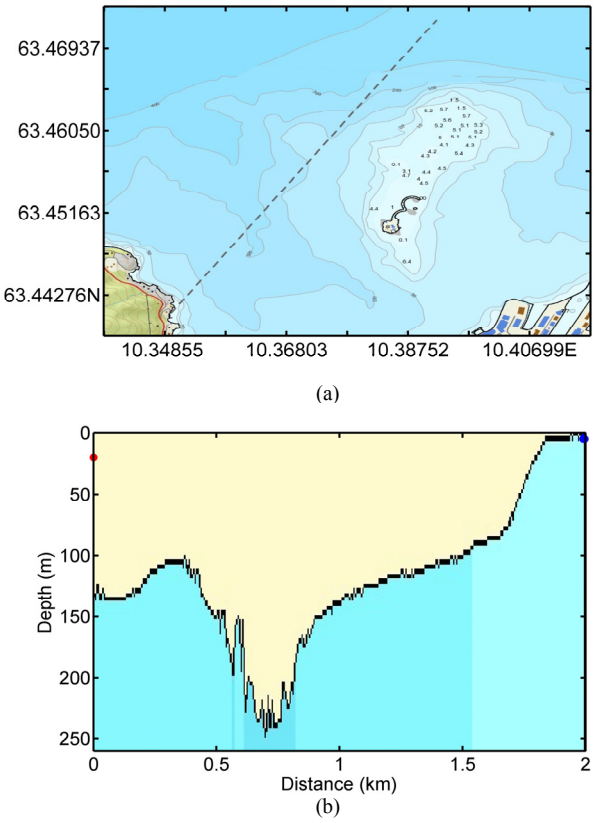

Figure 3. (a) Experimental area in Trondheim harbor. The dash line is the communication direction. (b) The depth profile in the communication direction. The red dot on the left denotes the transmitter position, and the blue dot on the right denotes the receiving array.

The sound speed profiles measured during the trials are shown in Figure 4. There was a sound channel at the depth of 25 m in Trial A. In Trial B, there was a negative gradient sound speed profile causing the acoustic energy emitted by the source bent towards the sea bottom. The receiving array was deployed at a depth which was different from the transmitter depth, and the received signal exhibited time-varying fading due to reflections from the sea surface and bottom.

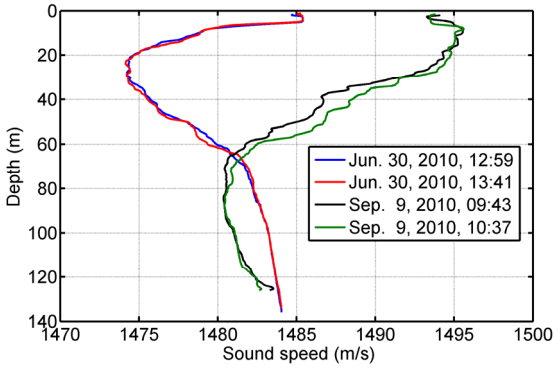

Figure 4. Sound speed profiles measured by Gunnerus.

The carrier frequency of the transmitted signals was 12 kHz. The channel probe signal was a linear frequency modulation (LFM) chirp of 0.1 s with a Hanning window, and its effective bandwidth was 2.2 kHz. The chirp was also used as a pulse-shaping signal for the data signals, which were generated by binary phase shift keying (BPSK), quadrature phase shift keying (QPSK) modulations. The symbol rate in communications was $R=1/T=1$ kilosymbols/s.

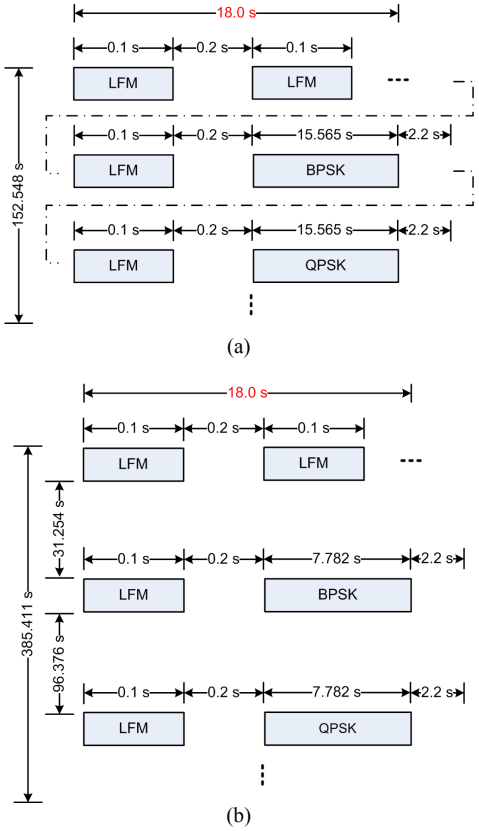

Figure 5. One period of the transmitted signal. (a) Trial A. (b) Trial B.

Figure 5(a) shows one period of transmitted signal for Trial A, where the signals were repeatedly transmitted 18

times. Figure 5(b) shows one period of transmitted signal for Trial B, where the signals were repeatedly transmitted 6 times. The 60 chirps spanning 18 s in each period were used to measure the channel response. The received waveforms were recorded with a sampling frequency of 96 kHz for off-line processing in the laboratory.

IV. THE RESULTS AND ANALYSIS

The parameters for PPC-DFE and PPC-McDFE are given in TABLE I. In baseband digital signal processing, the feed-forward filter taps span 4 symbol intervals with an over sampling rate of N=2. As suggested in [12], the second order DPLL is configured with $K_2=K_1/10$ to get good performance.

TABLE I. RECEIVER PARAMETERS

Parameters	Description	Value
F_s	The sampling frequency at the CRA	96 kHz
f_c	Carrier frequency	12 kHz
R	The symbol rate	1000 symbols/s
N	Over sampling factor	2
N_{ff}	The number of feed forward filter taps	8
N_{fb}	The number of feedback filter taps	2
N_t	The number of training symbols	72
λ	RLS forgetting factor	0.999
K	The number of receiving channels	10
K_1	Proportional tracking constant in PLL	0.01
K_2	Integral tracking constant in PLL	0.001

A. Trial A

In each period, the channel response within 18 s can be measured by the 60-chirp using the method of replica correlation. Figure 6 shows the overview of channel response measurements in hydrophone No. 4, which was located at a depth of 4.5 m above the sea bottom. The temporal compression is observed in the 45-minute trial, the time delayed arrivals in 18 periods are not aligned in delay time, and the first arrivals in the following periods approach the receiving array earlier than those in the previous periods. The compression rate changes with period, and the variation is caused by time-varying Doppler shift due to relative movement between the transmitter and the receiving array [13]. The channel response changes with time, it changes with receivers, and spatial diversity in the channel can be exploited to achieve stable communications.

Figure 7 shows the receiver performance in the first frame versus the number of hydrophones, where the output SNR is calculated by (1-MSE)/MSE [7]. The performance increases with the number of receiving channels, where spatial diversity is exploited, and PPC-McDFE achieves superior performance over PPC-DFE using a small number of receivers. In maximum, an improvement gain of 4.5 dB is obtained where the signals of 7 receiving channels are used for processing. In the following analysis, 10 receiving channels are used in signal processing to assess the improvement in terms of output SNR.

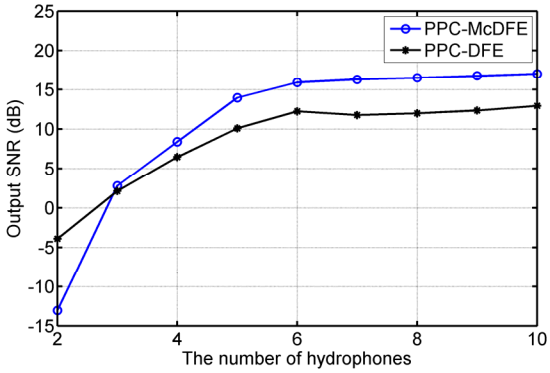

Figure 7. The performance for BPSK in terms of output SNR as a function of the number of receiving hydrophones.

In the 45-minute trial, Figure 8 shows that the receiver performance changes with time, and PPC-McDFE achieves better performance than PPC-DFE. Since the receivers were deployed in a region of reverberation, input SNR varied with time. It is shown in Figure 6 that magnitude of the arrivals changes with time in the trial. It is calculated that the improvement gain for BPSK communication changes from 2.2 dB to 6.7 dB and the improvement gain for QPSK communication changes from 2.5 dB to 6.4 dB. The reason for the improvement variation is that interchannel correlations exist and change with time.

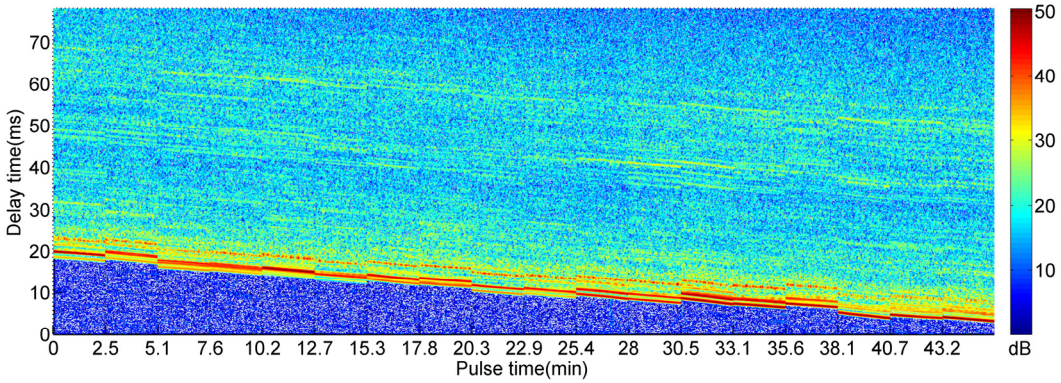

Figure 6. The channel impulse response measurements during the 45-minute experiment.

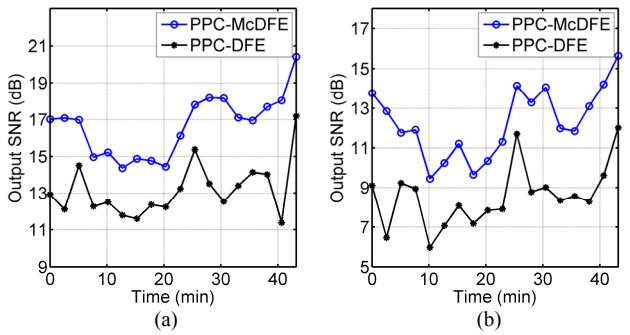

Figure 8. The performance in terms of output SNR. (a) BPSK. (b) QPSK.

Spatial coherence measures the strength of interchannel correlation between two receivers, and it can be calculated by

$$\psi(m,n)=\frac{\left|r_m(-t)\otimes r_n(t)\right|_{\max}}{\sqrt{\left|r_m(-t)\otimes r_m(t)\right|_{\max}\left|r_n(-t)\otimes r_n(t)\right|_{\max}}}, \quad (7)$$

where $\left|r_m(-t)\otimes r_n(t)\right|_{\max}$ denotes the maximum absolute value of cross-correlation between the two signals $r_m(t)$ and $r_n(t)$, and $r_m(t)$ denotes the signal received by the mth hydrophone. Figure 9 shows the spatial coherence measurement in the 45-minute trial, and interchannel correlation exists and changes with time during the trial. Since it is infeasible to predict the spatial coherence variations in a real ocean environment [9], it becomes intractable to preset weights for the multichannel combining. PPC-DFE assumes that there are independent receivers of the receiving array, where the spatial diversity is exploited by combining prior to the adaptive channel equalization, and this assumption is impacted by the interchannel correlations. PPC-McDFE achieves superior performance which is attributed to the adaptive spatial combining, as the multichannel combining weights are updated based on output MSEs.

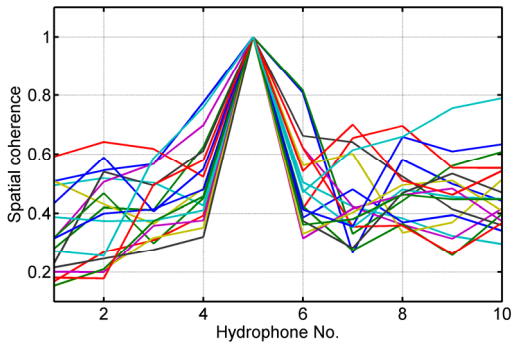

Figure 9. The spatial coherence as a function of the hydrophone index.

B. Trial B

Due to a negative gradient sound speed profile shown in Figure 4, extended time delayed arrivals caused by reflections are observed in Figure 10. The maximum magnitude decreases by 10 dB in the second period, and the compression due to Doppler is observed, where the compression rate is about 3.2e-4 between the two periods. Figure 11 shows the BPSK performance in the first period. There is no bit error of 7782 bits with an output SNR of 13.6 dB, and there is little difference in terms of the slope of phase offset from the DPLLs. This improvement gain is obtained from the adaptive spatial combining. The independent DPLLs are replaced by a common DPLL in the following processing

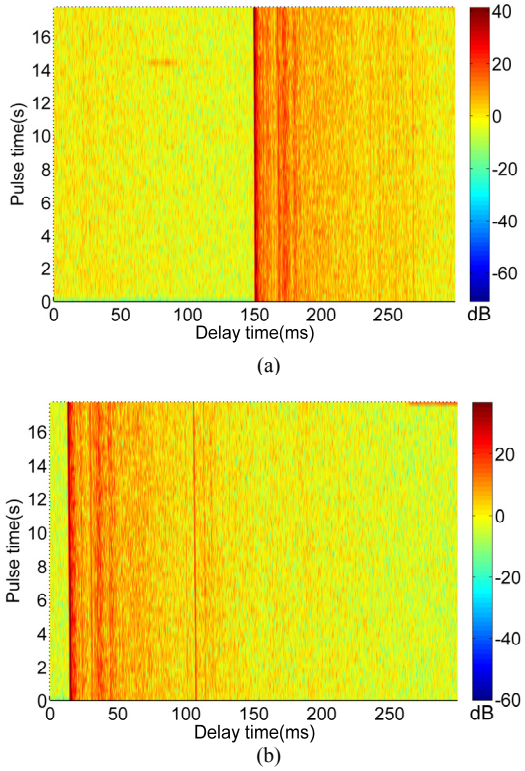

Figure 10. The impulse response measurements in two continuous periods within 385.411 s. (a) The first period. (b) The second period.

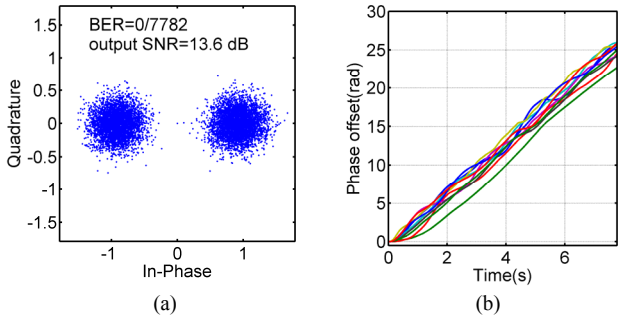

Figure 11. The receiver performance of PPC-McDFE. (a) The scatter plot. (b) The output of DPLL.

A single DPLL can update an averaged value of the phase-offset corrections among the 10 receivers, and it is given by

$$\bar{\hat{\theta}}[n] = \frac{1}{10}\sum_{i=1}^{10}\hat{\theta}_i[n] \quad (8)$$

where $\hat{\theta}_i[n]$ denotes the phase offset estimate from ith DPLL. Figure 12 shows the performance in 6 periods, and improvement of passive time reversal communications is obtained. In calculation, the improvement gain changes from 1.7 dB to 5.1 dB for BPSK, and it changes from 1.8 dB to 6.5 dB for QPSK. The improvement gain is attributed to spatial diversity exploited by the adaptive combining. Figure 13 shows the single DPLL output in 6 periods. For the BPSK signals, the slopes of phase offset change from 2.1 rad/s to 9.0 rad/s, where the equivalent carrier frequency shifts vary from 0.3 Hz to 1.4 Hz. The equivalent carrier frequency shifts for the QPSK signals change from 0.5 Hz to 0.9 Hz. In a time-varying acoustic channel, it is necessary that carrier-phase tracking by DPLL is implemented to compensate Doppler shift for underwater communications.

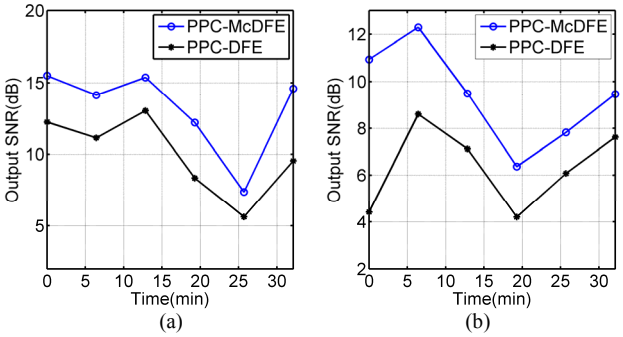

Figure 12. The performance in terms of output SNR. (a) BPSK. (b) QPSK.

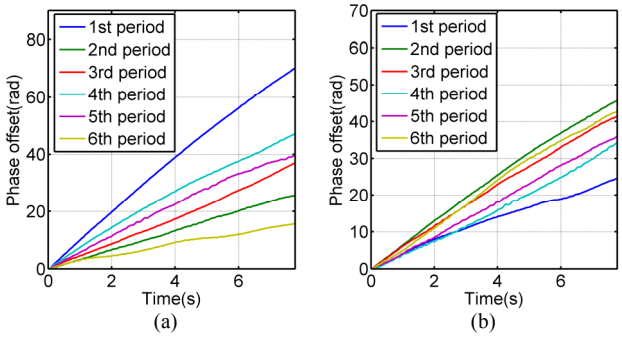

Figure 13. The single DPLL output. (a) BPSK. (b) QPSK.

V. CONCLUSIONS

The presented receiver structure which is based on pulse compression is assessed in two sea trials over a range dependent channel of 2 km. The presented results have shown that improvement of passive time reversal communications can be obtained by using adaptive spatial combining to exploit spatial diversity. In a real ocean, since the receivers of a receiving array are unable be distributed independently in space, there is no model which can predict time-varying interchannel correlations, and it is preferred that spatial diversity is exploited by the adaptive combining where the combining coefficients are updated to minimize output MSE. With a receiving array of a small number of hydrophones, we have demonstrated the performance of PC-McDFE.

ACKNOWLEDGMENT

The author would like to thank PhD students Zhongxi Chao, Yan Jiang, technical engineer Tim Cato Netland and the crew of the R/V Gunnerus for the help in conducting the experiments.

REFERENCES

[1] D. B. Kilfoyle and A. B. Baggeroer, "The state of the art in underwater acoustic telemetry," *IEEE J. Ocean. Eng.*, vol. 25, pp. 4-27, 2000.

[2] D. Rouseff, D. R. Jackson, W. L. J. Fox, C. D. Jones, J. A. Ritcey, and D. R. Dowling, "Underwater acoustic communication by passive-phase conjugation: theory and experimental results," *IEEE J. Ocean. Eng.*, vol. 26, pp. 821-831, 2001.

[3] G. F. Edelmann, T. Akal, W. S. Hodgkiss, K. Seongil, W. A. Kuperman, and S. Hee Chun, "An initial demonstration of underwater acoustic communication using time reversal," *IEEE J. Ocean. Eng.*, vol. 27, pp. 602-609, 2002.

[4] T. C. Yang, "Correlation-based decision-feedback equalizer for underwater acoustic communications," *IEEE J. Ocean. Eng.*, vol. 30, pp. 865-880, 2005.

[5] H. C. Song, W. S. Hodgkiss, W. A. Kuperman, M. Stevenson, and T. Akal, "Improvement of time-reversal communications using adaptive channel equalizers," *IEEE J. Ocean. Eng.*, vol. 31, pp. 487-496, 2006.

[6] D. R. Dowling, "Acoustic pulse compression using passive phase-conjugate processing," *J. Acoust. Soc. Am.*, vol. 95, pp. 1450-1458, 1994.

[7] J. G. Proakis, *Digital communications*. New York: McGraw-Hill, 2001.

[8] H. C. Song, W. S. Hodgkiss, W. A. Kuperman, W. J. Higley, K. Raghukumar, T. Akal, and M. Stevenson, "Spatial diversity in passive time reversal communications," *J. Acoust. Soc. Am.*, vol. 120, pp. 2067-2076, 2006.

[9] T. C. Yang, "A study of spatial processing gain in underwater acoustic communications," *IEEE J. Ocean. Eng.*, vol. 32, pp. 689-709, 2007.

[10] M. Stojanovic, J. Catipovic, and J. G. Proakis, "Adaptive multichannel combining and equalization for underwater acoustic communications," *J. Acoust. Soc. Am.*, vol. 94, pp. 1621-1631, 1993.

[11] S. Haykin, *Adaptive Filter Theory*. Upper Saddle River, New Jersey: Prentice Hall, 2001.

[12] M. Stojanovic, "Efficient processing of acoustic signals for high-rate information transmission over sparse underwater channels," *Physical Communication*, vol. 1, pp. 146-161, 2008.

[13] B. S. Sharif, J. Neasham, O. R. Hinton, and A. E. Adams, "A computationally efficient Doppler compensation system for underwater acoustic communications," *IEEE J. Ocean. Eng.*, vol. 25, pp. 52-61, 2000.

 ISBN: 978-1-61208-144-1